Effects of Shear-thinning and Elasticity in Flow around A Sphere in A Cylindrical Tube

Daoyun Song[*1], Rakesh K. Gupta[1], and Rajendra P. Chhabra[2]
[1]West Virginia University, [2]Indian Institute of Technology, Kanpur, India
*Corresponding author: Department of Chemical Engineering, West Virginia University, PO Box 6102, Morgantown, WV 26506, Daoyun.Song@mail.wvu.edu

Abstract: A sphere sedimenting in a cylindrical tube filled with non-Newtonian fluids, including purely viscous and viscoelastic type, is of both practical and fundamental interest. To investigate the effects of shear-thinning and elasticity, four representative constitutive equations are adopted, Newtonian, Carreau, Oldroyd-B and Phan-Thien-Tanner (PTT) models. There exists good agreement between our calculations and the prior results available in the literature. This lends credibility to the present approach in which the constitutive equation has been successfully implemented into COMSOL by the PDE mode. It was found that both the shear-thinning and elasticity lead to a decrease in the drag coefficient, while the velocity overshoot at the center line in the wake results from the interactions between the contributions of shear-thinning and elasticity.

Keyword: Carreau model, Phan-Thien-Tanner model, shear-thinning, viscoelasticity, sphere sedimentation in a cylindrical tube

1. Introduction

The motion of a sphere in a cylindrical tube filled with non-Newtonian fluids, including both purely viscous and viscoelastic type, has a broad range of practical applications including gravity-based separation techniques employed in chemical, mineral, and food processing, flow in fixed and fluidized bed reactors, falling ball viscometry and hydrodynamic chromatography, and sedimentation of muds and slurries and processing of filled polymer melts.[1,2] In addition to its practical applications, it is also of great fundamental and scientific significance. For instance, it may provide the basis of process design calculations. Apart from these considerations, this problem has also been one of the benchmark problems in the rheological numerical community.[3] This seemingly simple flow has defied satisfactory predictions due to immense computational difficulties arising from numerical instability, failure to converge at some critical high Weissenberg or Deborah numbers due to the existence of stress boundary layers, i.e., the so-called high Weissenberg or Deborah problem. This critical number depends on the flow configuration, selection of constitutive equation, discretization scheme of governing equations, mesh, stability scheme, order of interpolation function, and solver, etc.

The flow of both purely viscous and viscoelastic fluids past a sphere in a cylindrical tube has been studied by a vast number of researchers. For instance, Song et al.[1] have investigated systematically the flow problem of Newtonian and shear-thinning fluids (power law model). Chhabra et al.[4] have experimentally examined the flow of the Carreau model fluids over a sphere. Flow of viscoelastic fluids has also been explored widely using a range of constitutive relations, such as upper-convected Maxwell model (UCM)[5], Oldroyd-B[6] and Phan-Thien-Tanner model (PTT)[7], among many others. A good review regarding both transient and steady motion of a sphere in viscoelastic fluids has been given by McKinley.[2] To the best of our knowledge, however, there is no prior work which simulates the viscoelastic fluid flow around a sphere by means of COMSOL.

This work will investigate the effects of shear-thinning and elasticity on flow past a sphere in a tube with a fixed blockage ratio of d/D=0.5 in the limit of creeping flow (zero Reynolds number). Initially, the flow past a sphere immersed in a Newtonian fluid (constant viscosity without elasticity) is studied, followed by that of the Carreau model (shear-thinning without elasticity), and finally of the Oldroyd-B model (constant viscosity with elasticity) and the PTT model (shear-thinning with elasticity). The details of rheological model parameters used in this work are presented in the next section.

2. Governing equations

Consider a scenario in which a sphere with a

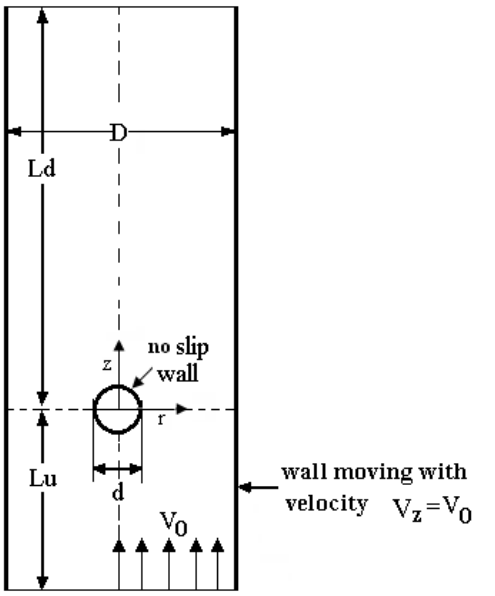

Figure 1. Schematic of flow around a sphere in a cylindrical tube

diameter *d* located at the axis of a cylindrical tube having a diameter *D* falls at a steady velocity V_0 in a tube filled with a quiescent liquid (purely viscous and viscoelastic). This situation is tantamount to the fluid moving at a uniform velocity of V_0 around the stationary sphere as shown schematically in Figure 1. Notice that the wall also moves upwards at the same velocity V_0.

For a two-dimensional, axisymmetric, steady flow in cylindrical coordinates, the governing equations in their compact forms are written as follows,

Continuity equation

$$\nabla \cdot u = 0 \tag{1}$$

Momentum equation in terms of stress (inertial effect is neglected)

$$-\nabla p + \nabla \cdot \sigma = 0 \tag{2}$$

where u is the velocity vector; p, pressure; σ, the extra stress. A constitutive equation is needed for the problem closure. In this work, four constitutive equations used herein include Newtonian fluid, Carreau fluid, Oldroyd-B and PTT models.

First, the Oldroyd-B model[8] is discussed.

$$\sigma + \lambda_1 \overset{\nabla}{\sigma} = \eta_0 \left(\dot{\gamma} + \lambda_2 \overset{\nabla}{\dot{\gamma}} \right) \tag{3}$$

in which λ_1 and λ_2 are the relaxation time and retardation time, respectively; η_0 is the zero-shear-rate viscosity, $\dot{\gamma} = \nabla u + \nabla u^T$. $\overset{\nabla}{\sigma}$ means the upper-convected derivative of the extra stress, defined by

$$\overset{\nabla}{\sigma} = \frac{D\sigma}{Dt} - \left(\nabla u^T \cdot \sigma + \sigma \cdot \nabla u \right)$$

$$= \frac{\partial \sigma}{\partial t} + (u \cdot \nabla)\sigma - \left(\nabla u^T \cdot \sigma + \sigma \cdot \nabla u \right) \tag{4}$$

One difficulty encountered in seeking a numerical solution to Eq. (2) is that it lacks the diffusivity term explicitly, which is conductive to augment the numerical stability. One possible remedy for this weakness is the approach based on the elastic viscous split stress (EVSS) technique, in which the extra stress is split into two terms, a viscous term and an elastic term as follows,

$$\sigma = \eta_N \dot{\gamma} + \tau \tag{5}$$

in which η_N is the Newtonian (solvent) viscosity. Substituting the above equation into Eqs. (2) and (3) yields

$$-\nabla p + \nabla \cdot (\eta_N \dot{\gamma}) + \nabla \cdot \tau = 0 \tag{6}$$

$$\tau + \lambda_1 \overset{\nabla}{\tau} = \eta_E \dot{\gamma} \tag{7}$$

where η_E is the elastic (polymer) viscosity,

$\eta_0 = \eta_N + \eta_E$, $s = \eta_N / \eta_0 = \lambda_2 / \lambda_1$

For the PTT model,[8]

$$\tau + \lambda_1 \overset{\nabla}{\tau} + \varepsilon \frac{\lambda_1}{\eta_E} tr(\tau)\tau = \eta_E \dot{\gamma} \tag{8}$$

in which ε is the extensibility parameter, resulting in the shear-thinning behavior and blunting the elongational singularity, tr(τ) is the trace of τ. When ε=0, Eq. (8) reverts to the Oldroyd-B model.

The Carreau model can be written as

$$\sigma = \eta_c \left(|\dot{\gamma}| \right) \dot{\gamma} \tag{9}$$

in which

$$\eta_c = \eta_0 \left[1 + \left(\lambda_c |\dot{\gamma}| \right)^2 \right]^{(n-1)/2}, \; |\dot{\gamma}| = \sqrt{\frac{1}{2} \dot{\gamma} : \dot{\gamma}} \tag{10}$$

where λ_c is a time constant, determining the point of onset of shear thinning, n is the power law index. When the shear rate approaches zero, it reduces to $\eta_c = \eta_0$ (a Newtonian fluid); when the shear rate is large ($\lambda_c |\dot{\gamma}| >> 1$), the well-known power-law model is recovered,

$$\eta_c = \left(\eta_0 \lambda_c^{n-1} \right) |\dot{\gamma}|^{n-1} = m |\dot{\gamma}|^{n-1} \tag{11}$$

Thus, this model is quite flexible in fitting viscosity data for most systems.

The flow curves predicted by the above mentioned constitutive equations are shown

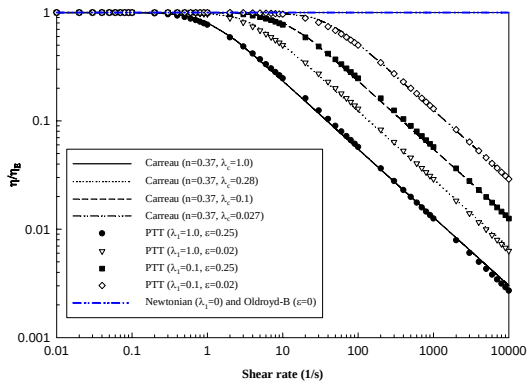

Figure 2. Shear viscosity curves predicted by four different types of constitutive equations

in Figure 2. Clearly, both the Carreau model and PTT model display the shear-thinning behavior, while the Newtonian and Oldroyd-B models have a constant viscosity. It is worth mentioning that ε=0.25 and 0.02 in the PTT model correspond to the flow behavior of two extremeities, concentrated polymer melts and dilute polymer solutions, respectively, meanwhile other parameters are chosen in such a way that the shear viscosity from Carreau model matches that from the PTT model (refer to the Appendix for details). Thus, Figure 2 demonstrates that the shear flow behavior of the Carreau model and the PTT model under these specific parameters is indistinguishable over the shear rate range of 6 decades. The model parameters are tabulated in Table 1. Since the flow of a sphere sedimenting in a tube is a hybrid of shear flow and extensional flow, i.e., at the center line, it is purely extensional and it is purely shear at the walls, it is also worth examining the elongational viscosities of the above mentioned constitutive equations as shown in Figure 3 (see Appendix for details). As can be seen from Figure 3, the Oldroyd-B model cannot represent the stretching behavior due to the stretching viscosity approaching infinity at some finite stretch rate. In addition, for the PTT model, a larger ε attenuates the extensional viscosity.

So far, the EVSS technique has been employed to enhance the numerical stability due to the hyperbolic type of the momentum equation. Similarly, the viscoelastic constitutive equations are of hyperbolic type, too. Therefore, some special algorithms are also required to improve the numerical stability. One popular algorithm is the so-called Streamline-Upwinding/Petrov-Galerkin method (SUPG)[9] and it was applied for this purpose. Since Eq. (7) is a special case of Eq. (8), only the SUPG on

Table 1. model parameters of PTT and Carreau

PTT model		Carreau model	
λ_1	ε	n	λ_c
1.0	0.25	0.37	1.0
	0.02		0.28
0.1	0.25		0.1
	0.02		0.027

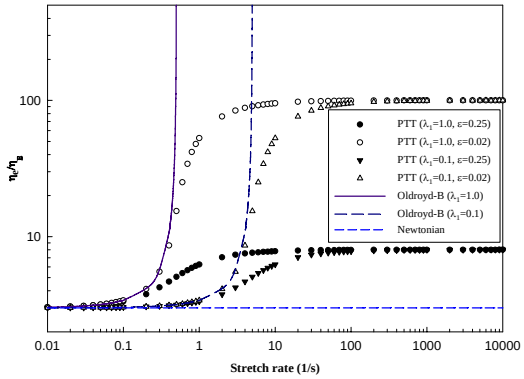

Figure 3. Extensional viscosity curves for different constitutive equations under the steady uni-axial flow

Eq. (8) was shown. The weighted residual forms solving the PTT model are as follows.

Find (u, p, τ) $\in V\times Q\times\Sigma$

$$\int_\Omega (\nabla\cdot u)q\, d\Omega = 0,\ \forall q\in Q$$

$$\int_\Omega \eta_N\left(\nabla u^T:\nabla v\right)d\Omega + \int_\Omega \tau:\nabla v\, d\Omega - \int_\Omega \nabla.v\ p d\Omega = 0$$

$$\forall v\in V$$

$$\int_\Omega \left[\tau+\lambda_1\overset{\nabla}{\tau}+\varepsilon\frac{\lambda_1}{\eta_E}tr(\tau)\tau-\eta_E\dot\gamma(u)\right]:\left(t+ku.\nabla t\right)d\Omega = 0$$

$$\forall t\in\Sigma$$

in which V, Q and Σ denote the function spaces for u, p and τ, respectively; v, q and t are weighting functions of u, p an τ, respectively, k ($h/\|u\|$) is the SUPG parameter; h is the element length, $\|u\|$ is the L^2 norm of the velocity vector.

Boundary conditions are as follows,

(1) Inlet

$$u_r = 0,\ u_z = V_0,\ \tau_{rr} = \tau_{rz} = \tau_{\theta\theta} = \tau_{zz} = 0$$

(2) Outlet

p=0, velocity is assumed to be fully developed.

(3) Symmetry

$$u_r = 0,\ \tau_{rz} = 0$$

(4) Sphere wall

$$u_r = u_z = 0$$

(5) Tube wall

$u_r = 0, u_z = V_0$

The Deborah number in this problem is defined by

$$De = \lambda_1 \bar{u} / R \quad (12)$$

A major quantity of interest is the drag force exerted on the sphere surface, calculated from the following equation,

$$F = \int_{\partial\Omega} [(-pI + \sigma) : n].e_z ds \quad (13)$$

in which n is the normal direction along the sphere surface, and e_z is the unit vector along the flow direction (z-direction here). The dimensionless drag coefficient factor of K is defined by

$$K = F / 6\pi\eta_0 \bar{u} R \quad (14)$$

3. Use of COMSOL Multiphysics

In this paper, the governing equations together with the appropriate boundary conditions have been solved using COMSOL Multiphysics (version 3.5a). The flow geometry was drawn by means of the built-in CAD tools, and the flow domain was meshed using "quadriclateral" elements. The built-in steady-state "Incompressible Navier-Stokes" and "Non-Newtonian Flow" modules were selected to solve for the flow of Newtonian and Carreau fluids. As for the viscoelastic fluid flow, although the current version of COMSOL Multiphysics (3.5a) does not offer a built-in module to handle this type of problem, several authors, Craven et al.[10] and Finlayson[11] successfully employed COMSOL to solve viscoelastic fluid problems. Here, we took advantage of the built-in module of incompressible Navier-Stokes equation to handle the momentum equation and continuity equation, while the constitutive equations were implemented into COMSOL by means of the PDE mode. Notice that some extra stress terms in the momentum equation were input through the body force terms. The scheme of Lagrange-P_2P_1 for velocity and pressure was selected to handle the velocity-pressure coupling, while the Lagrange-Linear scheme was applied to approximate the stress. These choices for velocity, pressure and stress satisfy the compatibility requirements or LBB (Ladyshenskaya-Babuška-Brezzi) condition. Direct UMFPACK and Parametric Solver were chosen. Once the flow domain was mapped in terms of the velocities, pressure and stresses, global characteristic quantities of interest, such as the drag coefficient, were obtained through post processing.

4. Results and Discussion

Before presenting our results, it is necessary to describe the choice of domain and mesh. Based on previous experience and guidance from the literature, the upstream Lu and downstream Ld were taken to equal 5d and 15d, respectively. A non-uniform, structured quadrilateral mesh was used. Additionally, the value of η_N / η_E chosen to be 0.05 (s=0.05/1.05) is a tradeoff between numerical stability and desire to reduce the Newtonian viscosity part influence.

4.1 Validation

To make sure that the implementation of the constitutive equation into COMSOL is correct, we first performed a simulation for the Oldroyd-B model at s=0.5. The drag coefficient obtained by us is compared to that reported by Lunsmann et al.[12] as shown in Table 2 and Figure 4. Obviously, present values are in exceedingly good agreement with the findings by Lunsmann et al. On the other hand, it is known that drag coefficient is a poor indicator of accuracy. A common way is to plot the normal stress component τ_{zz} along the sphere surface and the center line in the wake. Figure 5 shows the comparison of τ_{zz} between present computations and those due to Fan.[6] It is worth mentioning that Fan adopted an h-p adaptive technique to obtain very accurate solutions. As shown in Figure 5, our results show good agreement with values from Fan along the sphere surface. On the other hand, there exists a slight difference in the peak values between ours and Fan's along the downstream center line. It is not surprising at all to observe this difference at De=1.2. The reason is that once De exceeds some critical value, calculation of τ_{zz} at the downstream center line is extremely susceptible to the order of polynomial interpolation function and mesh as well, etc. Note that the highest order of interpolation functions employed by Fan is 8, whereas in our simulation, the orders of polynomial interpolation functions are 2, 1 and 1 to approximate velocity, pressure and stress, respectively.

4.2 Effects of Shear-thinning and Elasticity on Drag Coefficient

The drag coefficients predicted by the four

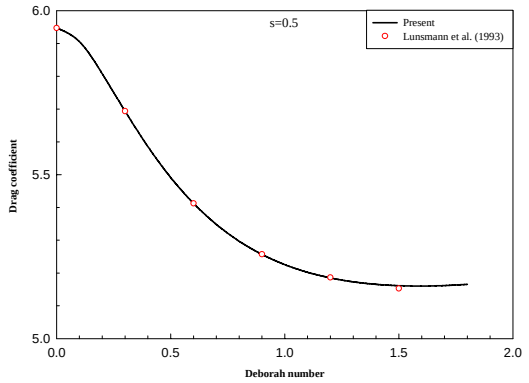

Figure 4. Comparison of drag coefficient of present computations and Lunsmann et al.[12]

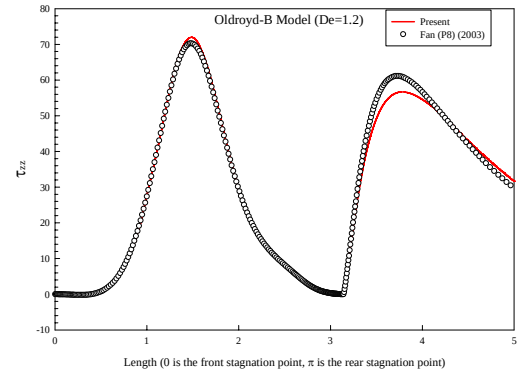

Figure 5. Comparison of stress along the sphere surface and the center line in the wake (P8 in Fan means that the highest order of polynomial interpolation functions in some elements is 8, s=0.5)

Table 2. Comparison of drag coefficient (s=0.5)

De	Present	Lunsmann et al.[12]
0	5.94739	5.94716
0.1	5.90562	
0.2	5.80781	
0.3	5.69385	5.69368
0.4	5.58553	
0.5	5.49107	
0.6	5.41221	5.41225
0.7	5.34805	
0.8	5.2968	
0.9	5.25654	5.25717
1.0	5.22548	
1.1	5.20205	
1.2	5.18493	5.18648
1.3	5.17297	
1.4	5.16536	
1.5	5.16132	5.15293
1.6	5.16025	
1.7	5.16171	
1.8	5.16535	

types of constitutive equations are presented in Figure 6. First, they decrease with the increase of De for the Oldroyd-B model. This suggests that elasticity reduces the drag coefficient. The two PTT models show the same trend as the Oldroyd-B model. Notice that for the PTT model, the decrease in drag coefficient is the result of both the elasticity and shear-thinning behaviors. As shown in Figure 6, the drag coefficient from the two PTT models is lower than that from Oldroyd-B. Further, the drag coefficient for the PTT model with ε=0.25 is the lowest compared to that from the other two viscoelastic models at the same De. This implies that shear-thinning behavior also leads to a reduction in drag coefficient. As shown in Figure 2, the PTT model with ε=0.25 possesses the smallest shear viscosity while all other conditions are identical. In addition, although the four dots representing Carreau model in Figure 6 exhibit the exactly same shear-thinning behavior as the PTT models, drag coefficients predicted by them are larger than those predicted by the corresponding PTT models. The reason behind this is the elasticity effect from the PTT model. In turn, this substantiates the conclusion that elasticity attenuates drag coefficient. Zheng et al.[7] also drew the same conclusion. Finally, the maximum attainable De for Oldroyd-B is 1.2 and 1.7 for PTT model with ε=0.02, respectively. The effort to get the maximum De for the PTT model with ε=0.25 was not made. At least, it should be greater than 2.0. This phenomenon may be interpreted by the shear and extensional viscosity curves as shown in Figures 2 and 3, respectively. At the same conditions, the PTT model with ε=0.25 always predicts the lowest shear and extensional viscosities, which yield the lowest stress as evidenced by Figure 7. It is the lowest stress that most likely delays the onset of

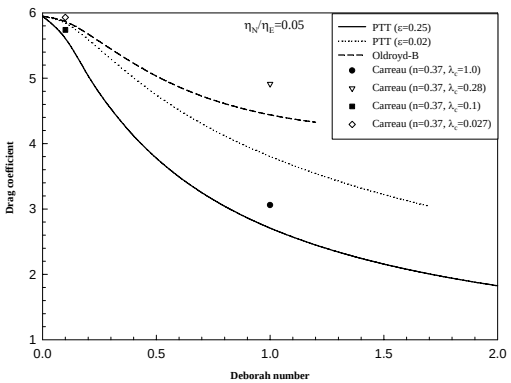

Figure 6. Drag coefficient obtained at different constitutive equations

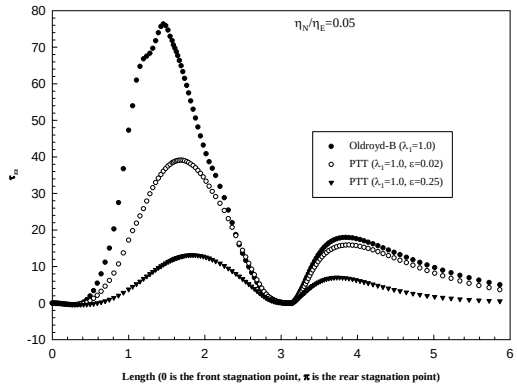

Figure 7. Comparison of τ_{zz} at λ_1=1.0 for Oldroyd-B and PTT models

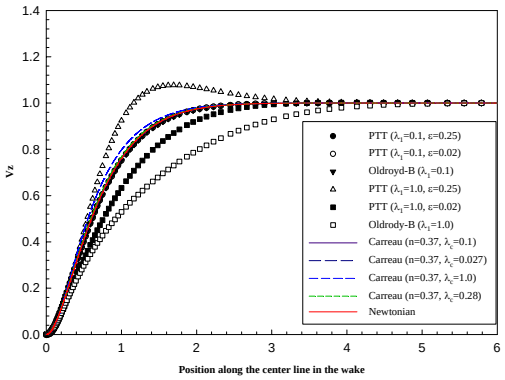

Figure 8. Velocity at the center line in the wake with $\lambda_1 \leq 1.0$

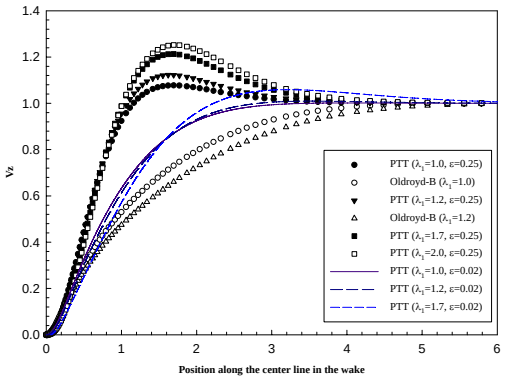

Figure 9. Velocity at the center line in the wake with $\lambda_1 \geq 1.0$

numerical method breakdown.

4.3 Effects of Shear-thinning and Elasticity on Velocity Overshoot

A conspicuous feature of the velocity curves at the downstream center line is the overshoot for the PTT model with λ_1=1.0 and ε=0.25 as shown in Figure 8. The overshoot feature has also been found numerically by Zheng et al.[7] and Jin et al.[13] Interestingly, there exists no overshoot predicted by either of the purely shear-thinning Carreau model and purely elastic Oldroyd-B model. As a result, the overshoot should be attributed to the synergistic effect of shear-thinning and elastic behaviors. Meanwhile, it is noted that there is no appreciable overshoot for the PTT model with ε=0.02. A further examination at higher λ_1 is shown in Figure 9. It reveals that there does exist an apparent overshoot for the PTT model with ε=0.02. However, the overshoot peak at ε=0.02 is not as prominent as that at ε=0.25. The exact reason is still unknown. Possibly, it may be interpreted by a lower extensional viscosity predicted by the PTT model with ε=0.25.

5. Conclusions

The governing equations for four representative fluids past a sphere in a cylindrical tube have been numerically solved using COMSOL. Flow of both the Newtonian and Carreau model fluids was solved by means of the built-in modules in COMSOL, while the viscoelastic models (Oldroyd-B and PTT) were implemented into COMSOL by the PDE mode. Our simulations for the Oldroyd-B model show good agreement with reports in the literature. Our calculations predict that both shear-thinning and elastic behaviors give rise to a reduction in the drag coefficient, whereas the synergistic influence of both of them results in the downstream velocity overshoot at the center line. The latter finding may suggest that the method of separation of elasticity and shear-thinning cannot always guarantee convergence or be justified. Finally, COMSOL has been successfully applied to solve viscoelastic fluid flow around a sphere in a tube.

6. References

1. D Song, RK Gupta, RP Chhabra, Wall effects on a sphere falling in quiescent power law fluids, *Ind. Eng. Chem. Res.*, **48**, 5845-5856 (2009).
2. GH McKinley, Steady and transient motion of spherical particles in viscoelastic liquids, in: *Transport Processes in Bubble, Drops, and Particles*; D De Kee, RP Chhabra, Eds, 2nd Ed., New York: Taylor & Francis, Chapter 14, pp 338-375 (2002).
3. Proceedings of the Fifth International Workshop on Numerical Methods in Non-Newtonian Flow, Lake Arrowhead, California, June 7-11, 1987

4. RP Chhabra, C Tiu, PHT Uhlherr, A study of wall effects on the motion of a sphere in viscoelastic fluids, *Can. J. Chem. Eng.*, 59, 771-775 (1981)
5. J Petera, A new finite element scheme using the Lagrangian framework for simulation of viscoelastic fluid flows, *J. Non-Newtonian Fluid Mech.*, 103, 1-43 (2002)
6. Y Fan, Limiting behavior of the solutions of a falling sphere in a tube filled with viscoelastic fluids, *J. Non-Newtonian Fluid Mech.*, **110**, 77-102 (2003)
7. R Zheng, N Phan-Thien, RI Tanner, The flow past a sphere in a cylindrical tube: effects of inertia, shear-thinning and elasticity, *Rheol. Acta*, **30**, 499-510 (1991)
8. RB Bird, RC Armstrong, O Hassager, *Dynamic of Polymeric Liquid*, Vol. 1, 2nd ed., New York: Wiley, 1987
9. JM Marchal, MJ Crochet, A new mixed finite-element for calculating viscoelastic flow, *J. Non-Newtonian Fluid Mech.*, **26**, 77-114 (1987)
10. TJ Craven, JM Rees, WB Zimmerman, Stabilised finite element modeling of Oldroyd-B viscoelastic flows, *COMSOL Conference*, Birmingham, UK (2006)
11. BA Finlayson, Using COMSOL Multiphysics to model viscoelastic fluid flow, *COMSOL Conference*, Boston, MA (2006)
12. WJ Lunsmann, L Genieser, RC Armstrong, RA Brown, Finite element analysis of steady viscoelastic flow around a sphere in a tube: calculations with constant viscosity models, *J. Non-Newtonian Fluid Mech.*, **48**, 63-99 (1993)
13. H Jin, N Phan-Thien, R.I. Tanner, A finite element analysis of the flow past a sphere in a cylindrical tube: PTT fluid model, *Comput. Mech.*, **8**, 409-422 (1991)

7. Acknowledgements

DS would like to thank Dr. Craven and Prof. Zimmerman from University of Sheffield and Prof. Finlayson from University of Washington for their help. We also would like to express gratitude to Prof. Fan from Zhejiang University for sending original data to us for quantitative comparisons reported here.

8. Appendix

In the simple steady shear flow field, PTT model can be simplified to

$$\tau_{xx}\left(1+\varepsilon\frac{\lambda_1}{\eta_E}\tau_{xx}\right)=2\lambda_1\tau_{xy}\dot{\gamma} \tag{A1}$$

$$\tau_{xy}\left(1+\varepsilon\frac{\lambda_1}{\eta_E}\tau_{xx}\right)=\eta_E\dot{\gamma} \tag{A2}$$

Eliminating τ_{xx} gives rise to

$$\tau_{xy}^3+A\tau_{xy}=B \tag{A3}$$

in which $A=\eta_E^2/2\varepsilon\lambda_1^2$, $B=\eta_E^3\dot{\gamma}/2\varepsilon\lambda_1^2$
One of its solutions is

$$\tau_{xy}=S-T \tag{A4}$$

where $S=\sqrt[3]{B+T^3}$, $T=\sqrt[3]{\frac{-B}{2}+\sqrt{\left(\frac{B}{2}\right)^2+\left(\frac{A}{3}\right)^3}}$

When ε=0, Eq. (A2) reduces to

$$\tau_{xy}=\eta_E\dot{\gamma} \tag{A5}$$

Thus, for the Oldroyd-B model, the shear rate viscosity is constant.

Under the steady state uni-axial extension, PTT model is reduced to

$$\tau_{xx}\left(1+\varepsilon\frac{\lambda_1}{\eta_E}tr(\tau)\right)=2\dot{e}\left(\lambda_1\tau_{xx}+\eta_E\right) \tag{A6}$$

$$\tau_{yy}\left(1+\varepsilon\frac{\lambda_1}{\eta_E}tr(\tau)\right)=-\dot{e}\left(\lambda_1\tau_{yy}+\eta_E\right) \tag{A7}$$

where $tr(\tau)=\tau_{xx}+2\tau_{yy}$, stretch rate $\dot{e}$, $=\partial u_x/\partial x$

$$\tau_{yy}=-\frac{\eta_E\tau_{xx}}{3\lambda_1\tau_{xx}+2\eta_E} \tag{A8}$$

Substituting Eq. (A8) into Eq. (A6) yields

$$\tau_{xx}^3+a\tau_{xx}^2+b\tau_{xx}+c=0 \tag{A9}$$

$a=\frac{(1-2\lambda_1\dot{e})\eta_E}{\varepsilon\lambda_1}$, $b=\frac{2(1-5\lambda_1\dot{e})\eta_E^2}{3\varepsilon\lambda_1^2}$, $c=-\frac{4\eta_E^3\dot{e}}{3\varepsilon\lambda_1^2}$

One of its solutions is,

$$\tau_{xx}=2\sqrt{\frac{|P|}{3}}\cos\left(\frac{\phi}{3}\right)-\frac{a}{3} \tag{A10}$$

$P=b-\frac{a^2}{3}$, $Q=c+\frac{2a^3-9ab}{27}$, $\phi=\arccos\left(-\frac{Q}{2\sqrt{|P|^3/27}}\right)$

The extensional viscosity is defined by

$$\eta_{\dot{e}}=\frac{\tau_{xx}-\tau_{yy}}{\dot{e}} \tag{A11}$$

When ε=0 (Oldroyd-B), the stretch viscosity equals

$$\eta_{\dot{e}}=\eta_E\left(\frac{2}{1-2\dot{e}\lambda_1}+\frac{1}{1+\dot{e}\lambda_1}\right) \tag{A12}$$

Further, as λ_1 =0 (Newtonian fluid), the Trouton's ratio of $\eta_{\dot{e}}/\eta_E=3$ is recovered.